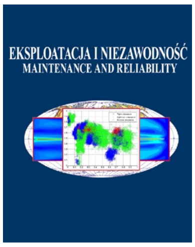

Eksploatacja i Niezawodnosc – Maintenance and Reliability
Volume 24 (2022), Issue 4
journal homepage: http://www.ein.org.pl
Article citation info:
Michnej M, Młynarski S, Pilch R, Sikora W, Smolnik M, Drożyner P. Physical and reliability aspects of high-pressure ammonia water pipeline failures. Eksploatacja i Niezawodnosc – Maintenance and Reliability 2022; 24 (4): 728–737, http://doi.org/10.17531/ein.2022.4.13

Physical and reliability aspects of high-pressure ammonia water pipeline failures

Indexed by: Web of Science Group

Maciej Michnej[a], Stanisław Młynarski[a], Robert Pilch[b], Wojciech Sikora[b], Maksymilian Smolnik[b], Przemysław Drożyner[c]

[a] Cracow University of Technology, Faculty of Mechanical Engineering, al. Jana Pawła II 37, 31-864 Kraków, Poland
[b] AGH University of Science and Technology, Faculty of Mechanical Engineering and Robotics, al. Mickiewicza 30, 30-059 Kraków, Poland
[c] University of Warmia and Mazury in Olsztyn, The Faculty of Technical Sciences, ul. Oczapowskiego 11, 10-719 Olsztyn, Poland

Highlights

- The research problem was to determine the cause of the damage of the pipeline.
- Several tests of different types of selected parts of the pipeline were carried out.
- Structural analysis of the pipeline compensators was conducted.
- An attempt was made to develop a reliability model of the tested object.
- Practical recommendations on pipeline safe operation were made.

Abstract

The paper concerns the problem of the occurrence of failures of the high-pressure ammonia water pipeline of the coke oven battery complex, which is affected by chemical and thermal factors as well as the operating pressure occurring during its use. Pipeline failures manifested themselves as leaks (leakage of the medium) due to cracks in the area of the pipeline thermal elongation compensators. The conducted tests included, among others: visual inspection, penetration tests, macroscopic and microscopic tests as well as chemical analysis of the material. The study includes microscopic photographs of the material structure and cracks. The results of the pipeline strength and reliability analysis were also presented. On the basis of the conducted research and analyses conclusions were formulated. The assumed cause of the damage was the incorrectly made welded joints. Formulated recommendations and proposals for actions aimed at avoiding further failures of this and similar pipelines were related to the inspection time and preventive renewal.

Keywords

coke oven battery, pipeline, welded joint, crack, structural analysis, reliability assessment.

1. Introduction

The use and maintenance of complex and operating in difficult conditions technical systems always carries the risk of both forms of wear and failures [5, 6, 21], which the operator did not expect. Such failures, occurring at unforeseen moments, cause the greatest difficulties, often long downtimes increasing financial losses and may pose a threat to people and the environment [11].

The causes of this type of failures may result from errors made at the design stage of the system, e.g. incorrect selection of materials or imperfections of the calculation models used. It is also often impossible to precisely determine the operating conditions, the range of variability of all factors, their impact force and interaction on the object being designed [7]. The reason for the occurrence of unforeseen failures may also be undetected defects in materials and errors in the production process of the objects which constitute the technical system [12]. A failure may be caused by inaccuracies and technological errors made during the final assembly of the system in its target place of operation, where the conditions for the performance of works are far from ideal. The multitude of causes and possibilities leading to the appearance of unexpected failures of objects during their operation means that despite various attempts and treatments, it is not possible to eliminate them and in practice, the possibility of their occurrence should always be taken into account (see [8, 13, 22]).

One of the frequently appearing and analysed problems is corrosion and cracking of pipelines transporting a medium with high temperature and an adverse effect on the pipeline material [3, 16]. The areas of welded joints and sections of pipeline change of direction are particularly vulnerable to damage in these facilities. Welded joints are critical areas in the structure. Damage in this area has been reported many times [1, 2, 14, 15] and is a problem related to stress in and strength of the construction material. Differences in the hardness of the pipeline components can cause damage initiation in the connection area [18].

The study presents the problem and analysis of the failures of a pipeline, the unusual damage of which occurred unexpectedly during its initial operation.

E-mail addresses: M. Michnej (ORCID: 0000-0003-0030-1973): maciej.michnej@pk.edu.pl, S. Młynarski (ORCID: 0000-0002-3374-7739): mlynarski_st@poczta.onet.pl, R. Pilch (ORCID: 0000-0003-2342-5776): pilch@agh.edu.pl, W. Sikora (ORCID: 0000-0002-2953-5653): wosikora@agh.edu.pl, M. Smolnik (ORCID: 0000-0003-0753-5190): smolnik@agh.edu.pl, P. Drożyner (ORCID: 0000-0002-6125-8035): przemyslaw.drozyner@uwm.edu.pl

The aim of the work is to identify the failures of the pipeline, analyse their potential causes and attempt to develop a description of reliability of the tested object. The obtained characteristics may be helpful in the assessment of technological solutions applied in the considered operating conditions.

2. Characteristic of the examined object

The object of the study is the high-pressure ammonia water pipeline of the coke oven battery complex. The pipeline is placed on sliding supports with certain movement restrictions and fixed supports. The supporting elements are brackets connected with the trestle bridge common to two other process pipelines. The entire route of the pipeline runs with a slope of 3 ‰ to 8 ‰ between successive supports. The pipeline is operated in the natural ambient conditions of the coke oven battery. The pipeline components are protected against weather conditions with a varnish coat. The ambient temperature of the pipeline is defined as being between -25°C in winter and + 30°C in summer. The structure of the pipeline ensures compensation of changes in its length due to temperature changes. Length change compensators were made by local U-shaped profiling of the pipeline (Fig. 1), which allows for compensation of the length by elastic deformations of the pipeline material within such a section. Solutions of this kind are commonly applied and usually do not cause operational problems. However, in the analysed case, pipeline leaks were observed in the area of the mentioned compensators. The first to be analysed are the factors related to the environment and the operating parameters of the pipeline.

Fig. 1. View of a part of the ammonia water pipeline

Operation of the pipeline is carried out under the conditions defined by:

- corrosivity of the environment described by category C4 according to PN-EN ISO 12944,
- maximum operating pressure – 5,5 MPa,
- opearting temperature – approximately 80°C.

After about two years of operation of the pipeline, liquid drops was observed in the area of thermal elongation compensators. The analysis of the condensate and the place of its appearance revealed the pipeline cracks and the leakage of the transported medium. The damages were found around characteristic points of the pipeline compensators. The formation of new cracks in the area of already existing damage was also observed. Due to the need for uninterrupted use of the pipeline, attempts were made to repair the pipeline in damaged places on an ad hoc basis by covering the leaky parts with additional tight external bands. The process of the failures occurrence was subjected to appropriate tests.

3. Localisation of the pipeline damage

The failures of the high-pressure ammonia water pipeline of the coke oven battery complex consisted of leaks (medium leaks) caused by cracks in the pipeline thermal elongation compensators, appearing on welded joints and in their immediate vicinity. The analysis of the time of occurrence of the pipeline failures showed that most of them took place during 5 months of the pipeline's operation, after about two years of its use. All the failures occurred in the area of the joints of the bends constituting parts of the pipeline compensators. Fig. 2 shows a scheme of the pipeline route and additionally marked the characteristic places where the damage was located.

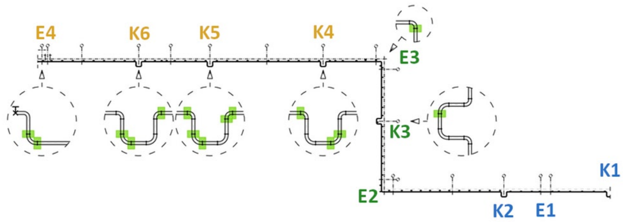

Fig. 2. Scheme of the pipeline with marked compensators (K1-6) and changes to its route (E1-4) [10]

The location of the damage may indicate the relationship of their formation with the local nature of the operation of a compensator profile. However, as schown in the scheme, the damage was not found in all of the affected areas. Therefore, the pipeline components were further tested.

4. Tests and their results

First, information was collected on the operating time of the pipeline during which the considered failures occurred. Subsequent tests were aimed at verifying the primary indications of causes and showing other possible causes of failures.

Further tests of the pipeline included an external visual inspection, during which the damaged elements were checked and the scope of the damage was determined. Then, penetrant tests, macroscopic tests, microscopic tests as well as chemical analysis and hardness measurements of the construction material of the elements were carried out. The welds, bends and pipe sections from the part of the high-pressure ammonia water pipeline supplied for testing were examined. Macroscopic examination and observation also concerned the remaining pipeline compensators.

4.1. External examination, penetration tests and macroscopic tests

Figures 3 and 4 show selected pipeline welds tested, marked with symbols A1, B1 and C1. There were sealing bands on the welds placed on the pipeline during its operation after the occurrence of leakage. The joint A1 was sealed with a double flange with an external band.

The sections of the pipeline with the welded joints were cut longitudinally and a part of the pipeline was cut out of the external band. Then, the parts of the pipeline in the weld zone were cleaned of paint and impurities for testing. Fig. 5 shows the parts of the A1 weld from the root side. The arrow marks the visible crack in the pipeline wall. Penetrant testing was performed to reveal any other cracks not visible to the naked eye.

Figures 6 and 7 show the pipeline cracks visible from the inside, detected by penetrant tests. Dye penetrant has leaked to the outside of the pipe in some places.

Fig. 8. shows a part of the pipeline with C1 joint after it has been cut open. Fig. 9 shows the pipeline cracks visible from the inside, detected by penetrant tests

The welded joints in the area of which cracks were revealed were cut transversely and examined after etching. The existing cracks in the

Fig. 3. A1 joint of the high-pressure ammonia water pipeline

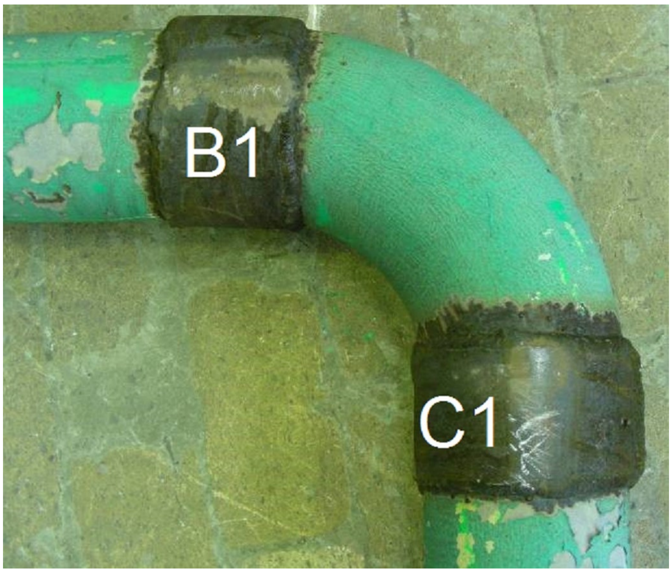

Fig. 4. B1 and C1 joints of the high-pressure ammonia water pipeline

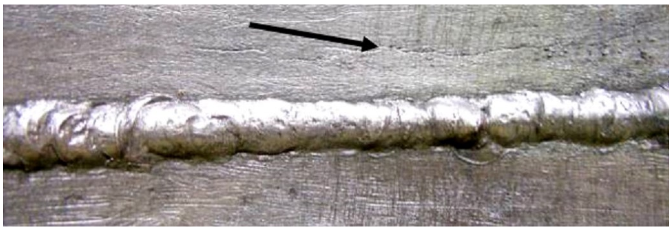

Fig. 5. View of the A1 welded joint from the root side (from the inside of the pipe)

material of the pipeline in various places around the welded joints A1 and C1 are shown in Fig. 10. These cracks are located in the material outside the joint.

All the cracks in the pipeline near the joints were located in its bends and propagated from the inside of the pipeline. Where the crack reached the outer surface of the pipe, the medium penetrated the gap and the pipeline began to leak. Defects of joints visible in the cross-sections, such as shifts of the joined edges, may be of significant importance for the operation of the joint and the occurrence of the observed defects.

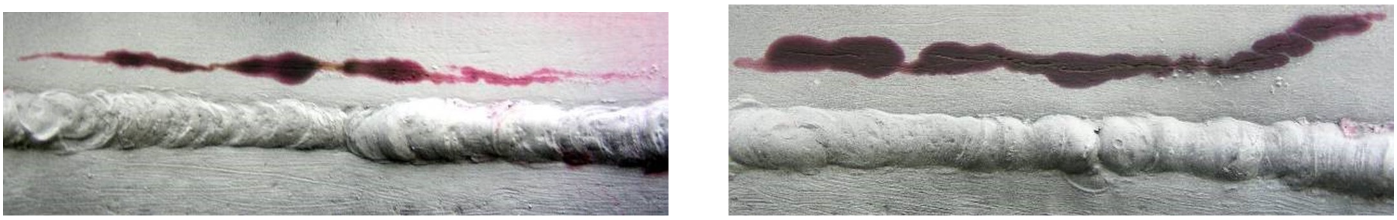

Fig. 6. View of the A1 welded joint from the root side after penetrant testing

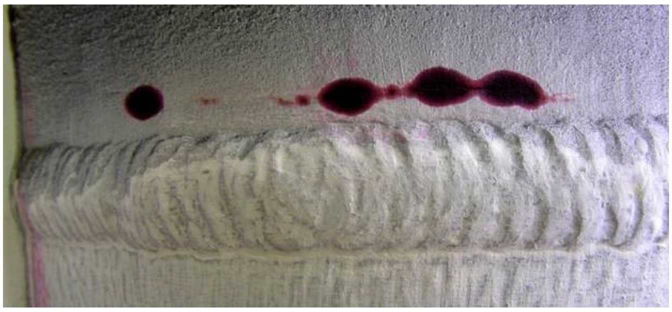

Fig. 7. View of the A1 welded joint from the face side after penetration of the dye penetrant from the inside of the pipe

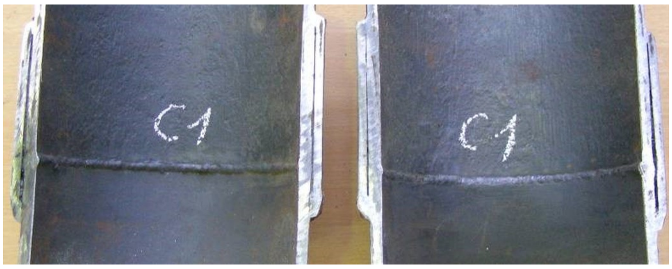

Fig. 8. View of C1 welded joint from the root side; visible sealing band

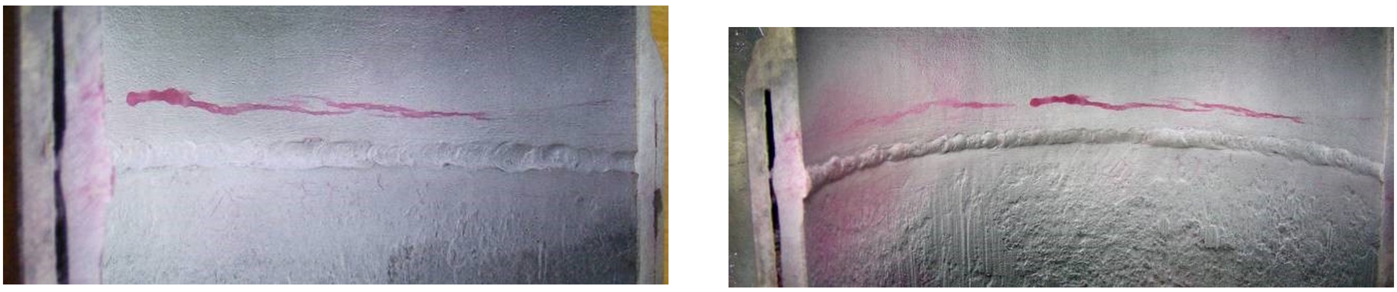

Fig. 9. View of the C1 welded joint from the inside of the pipeline after penetration testing

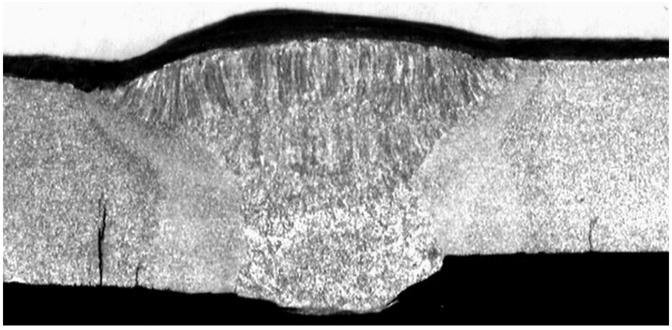

Fig. 10. Cross-sections of A1 (left) and C1 (right) welded joints

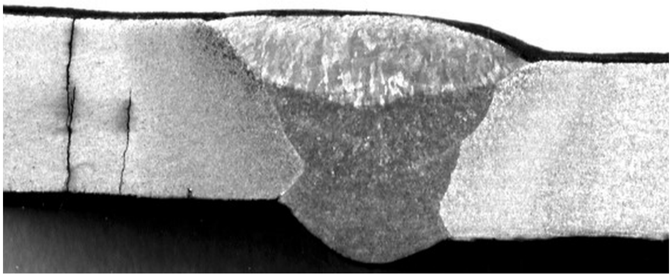

Fig. 11. Structure of the pipe material. 100x magnification, nital etching

4.2. Metallographic examination

The examination of the material structure of the pipeline elements was carried out on metallographic specimens obtained from parts of pipes and bends. The aim of the study was to identify the material from which the individual elements of the pipeline had been manufactured. The identification of the structure was necessary to further verify the causes of the failures. The structure of the pipe material is shown in Fig. 11 and 12 at magnifications of 100x and 500x. The observed structure was ferritic-pearlitic. The particles of perlite were lamellar. There were no irregularities in the examined structures in the form of inclusions or discontinuities.

Fig. 13 to 16 show selected damage cases observed in the bend material near the A1 and C1 welded joints.

4.3. Chemical analysis of the material

The chemical analysis of the material of the pipeline elements was carried out applying the spectral method. It was necessary to infer about the causes of the damage. The chemical composition has a significant impact on the physical and chemical properties of the material, which in the discussed case were highly relevant to the damage process. The test results are presented in Tab. 1. The table shows the chemical composition of the material from which the pipeline was made (requirements grade 1 boiler pipes) according to the Factory

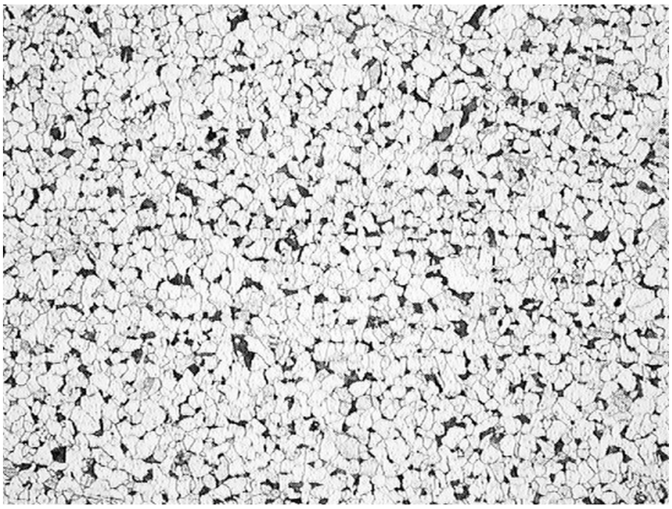

Fig. 12. Structure of the pipe material. 500x magnification, nital etching

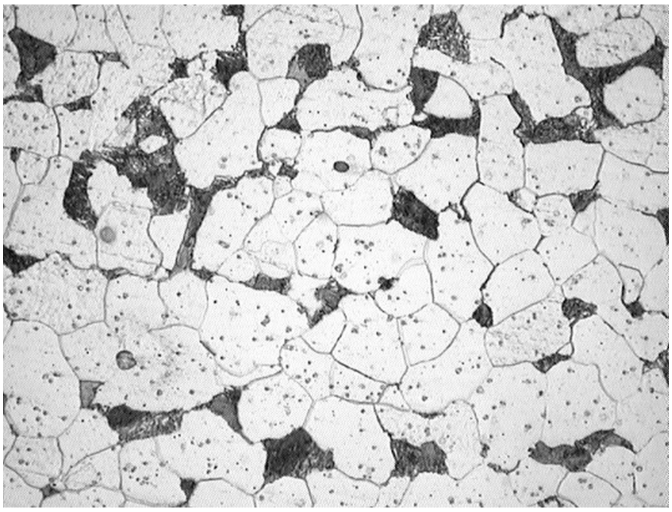

Fig. 13. Crack in the bend material in the vicinity of the A1 welded joint. Approx. 2,5x magnification, nital etching

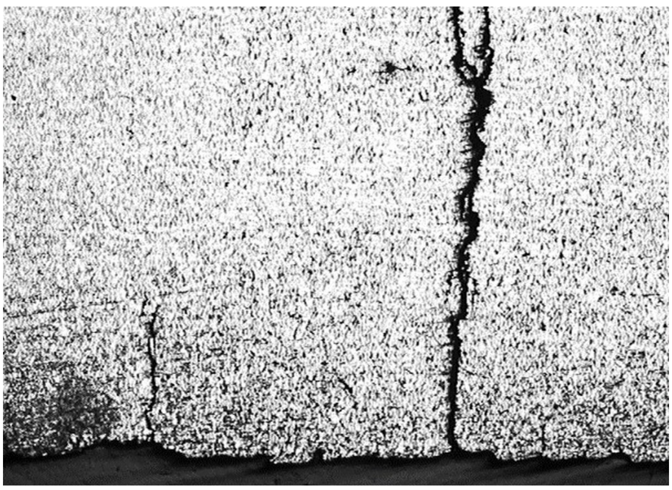

Fig. 14. Crack in the bend material in the vicinity of the A1 welded joint. 100x magnification, nital etching

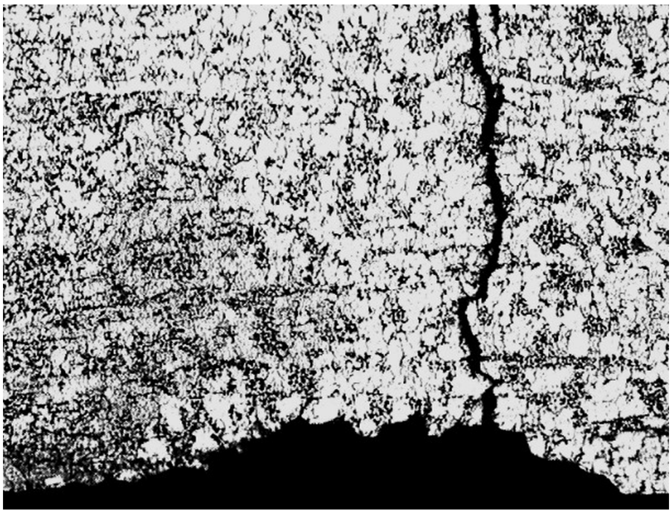

Fig. 15. Crack in the bend material in the vicinity of the C1 welded joint. Approx. 50x magnification, nital etching

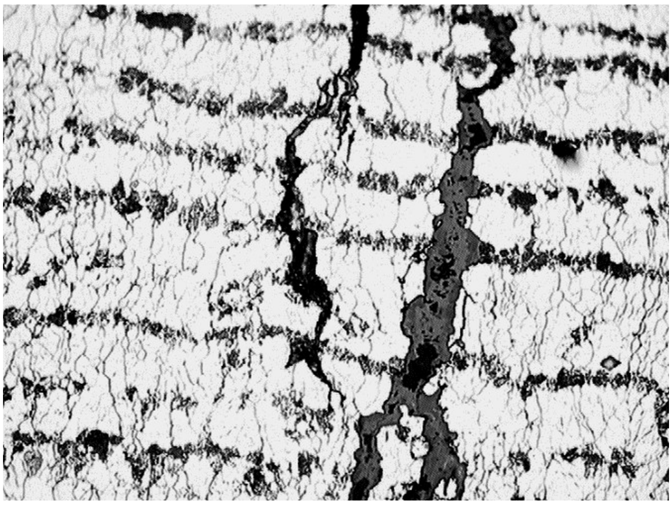

Fig. 16. Crack in the bend material in the vicinity of the C1 welded joint. Approx. 500x magnification, nital etching

change by an angle 90°. Indicated locations along the pipeline were investigated through structural mechanics calculations.

To assess a level of nominal stress within the pipeline and rule out basic design errors, the pipeline model was prepared in the ANSYS simulation environment based on the finite element method. Using elements PIPE289 and ELBOW290, dedicated for piping calculations, its route was recreated. FEM analysis was performed under assumptions of a static and linear system. The pipeline geometry change due to deformation did not have significant effect on the obtained results. The assumed boundary conditions were as follows: outermost nodes, at the start and end of pipeline, were fixed. At locations of the pipe intermediate physical supports (80 in total), nodes were constrained in directions perpendicular to the pipeline axis. Supports were located according to the technical documentation of the pipeline. Working loads were applied in the form of internal pipe pressure equal to 5.5 MPa and internal temperature of +80°C, both compliant with the documentation.

The major factor contributing to the stress within the pipe are thermal strains. Their magnitude depends of an environmental (reference) temperature and temperature gradient across pipe wall thickness. Final external pipe temperature can reach different values as it depends on the pipe surface emissivity and, also, environmental temperature. Therefore in the performed analysis a possible range of the pipe outer surface temperature was considered (Fig. 18 and 19) which allowed to obtain a potential range of stress occurring in the pipeline. Calculations were conducted for two different environment temperatures: +20°C and −20°C. Due to higher difference between the temperatures in the regard to a transported medium, higher mean stress was observed for the second variant.

Table 1. Chemical compositions of the steel

	C	Mn	Si	P	S	Cr	Ni	Cu	Mo	Nb	V	Al	N_2	B
	Content in %													
3.1.B	0.14	0.48	0.22	0.012	0.008	0.05	0.09	0.15	0.014	0.002	0.002	0.025	0.0084	0.0001
A1	0.23	0.50	0.27	0.015	0.010	0.02	0.03	0.06	0.01	0.002	0.001	0.001		
B1	0.16	0.95	0.26	0.015	0.005	0.03	0.01	0.02	0.00	0.004	0.003	0.033		
C1	0.21	0.45	0.25	0.015	0.020	0.05	0.03	0.13	0.01	0.002	0.006	0.001		
P235GH	max. 0.16	max. 1.20	max. 0.35	max. 0.015	max. 0.020	max. 0.30	max. 0.30	max. 0.30	max. 0.08	max. 0.010	max. 0.02	max. 0.020		max. 0.0001
P245GH	0.08 0.20	0.5 1.3	max. 0.40	max. 0.025	max. 0.015	max. 0.30								
P250GH	0.18 0.23	0.30 0.90	max. 0.40	max. 0.025	max. 0.015		max. 0.30	max. 0.30		max. 0.010	max. 0.02	0.015 0.050		

Acceptance Certificate (3.1.B). The table also shows the chemical composition of steel grade P235GH, material number 1.0345 according to PN-EN 10216-2 (old marking St36K according to PN/H-84024 from 1975).

All sections of the tested pipes are made of steel of chemical composition corresponding to the chemical composition of steel grade P235GH.

The material of the bends has a chemical composition corresponding to the chemical composition of steel grade P245GH and material number 1.0352 according to DIN 102222-2 and PN-EN 10222-2 and P250GH material number 1.0460 according to DIN 17243 and PN-EN 10222-2.

As a result of the analysis, the chemical composition of the tested material in the vicinity of A1, B1 and C1 joints was determined. The results presented in the table are in accordance with the adopted standards and recommendations for materials used in the construction of ammonia water pipelines.

5. Structural analysis of the pipeline compensators

Pipeline route changes its direction twice, in both cases by an angle of 90°, thus it creates three straightforward segments. In each of them, there are compensators located marked by the letter ''K'' (Fig. 2) and three different colours, depending on which of the segments they are situated. Similarly marked, but with letter ''E'', are local route changes. Positions E1 and E4 refer to slight pipeline bypasses necessary because of a pre-existing infrastructure in the given area. Remaining positions E2 and E3 are the result of the pipeline main route direction

The example of the stress distribution in K2 compensator for environmental temperature and pipe outer surface temperature equal to −20°C is shown in Fig. 17. This stress results from the normal stress coming from bending and tension/compression. The figure shows its maximum value in a given location along pipeline axis. In each of the compensators, the stress distribution is very similar as in Fig. 17. The highest values can be observed in bends located by the main pipeline. Calculated specific values are, however, varied and dependent on which of the three pipeline segments given compensator is located.

Based on Fig. 18 and 19, which present the maximum values of stress in locations K and E as a function of temperature of the pipe outer surface, it can be observed that compensators K4-6 are loaded almost in the same way and stress level there is significantly lower compared to the rest of compensators. Next, according to the ascending load order, are compensators K3, K1 and K2. Higher value of stress in these pipeline parts can be explained through the lower number of compensators in the regard to the length of the given pipeline segment. In all these locations and for all temperature variants, maximum stress did not exceed yield stress for steel P235GH ($Re \approx 235\,\text{MPa}$)

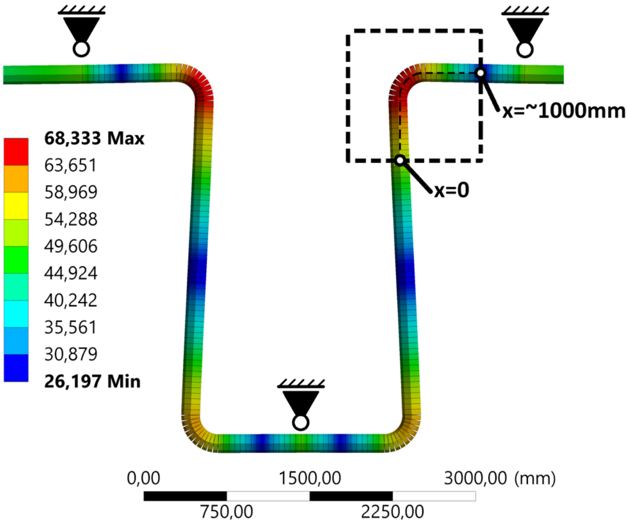

Fig. 17. Equivalent stress [MPa] distribution in the K2 compensator for the environmental temperature and pipe outer surface temperature both equal to −20°C. *Intermediate supports locations are showed. Visible deformation is scaled. Dashed rectangle shows pipeline part from Fig. 20*

from which pipes were manufactured. They remained at a safe level (max. 140 MPa). For locations marked as E, stress values were comparable with those in the compensators.

The stress distribution in the vicinity of a single bend of the compensator K2 (Fig. 2) is showed in Fig. 20. The stress is plotted as a function of the pipe length measured along its route. Maximum stress occurs within the bend, but a bit further from it, in both directions, where the actual welded joints are located, the stress is significant lower. More sharp decline appears in case of the part located on the main pipeline route, which is caused by a close proximity of the pipe support. Therefore, actual value of the stress in the place where welded joints are located should be even lower that it was initially estimated in Fig. 18 and 19.

Possible mechanism behind the failures of the investigated pipeline can be material fatigue. According to the information delivered by the operator, once per day the temperature inside pipes is decreasing to, approximately, an environmental temperature. It can be interpreted as a single cycle of a thermal load of the pipeline. The number of 365 cycles per year resulting from this, excludes possibility of material fatigue occurrence with an exception of a situation when stress in the pipes would exceed the yield stress and it could lead to a low cycle fatigue.

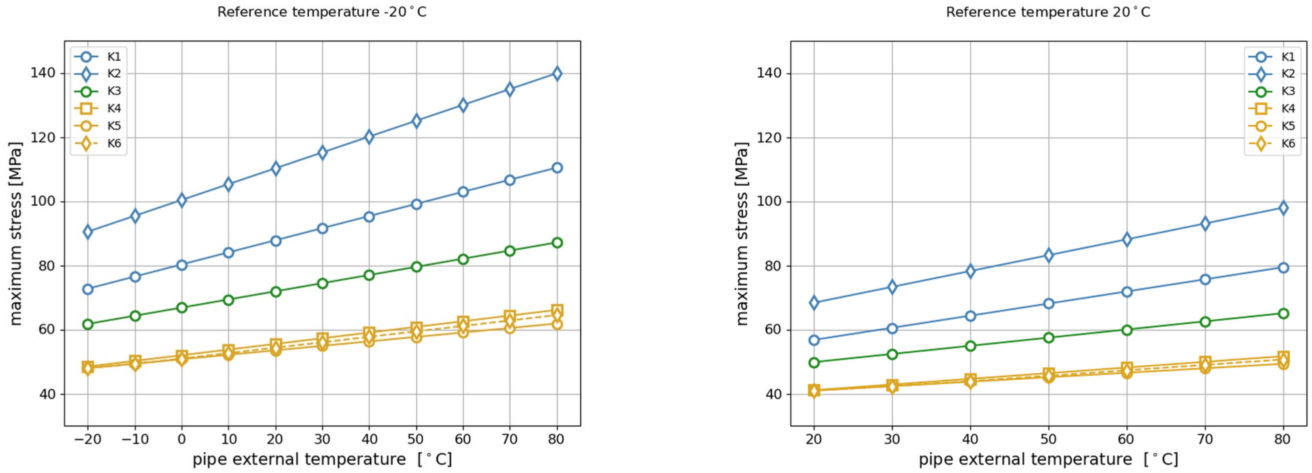

a) for T_{env}=−20°C *b) for* T_{env}=20°C

Fig. 18. Maximal equivalent stress [MPa] in pipeline compensators, as a function of pipe outer surface temperature for environmental temperature a)−20°C −20°C*, b)* 20°C

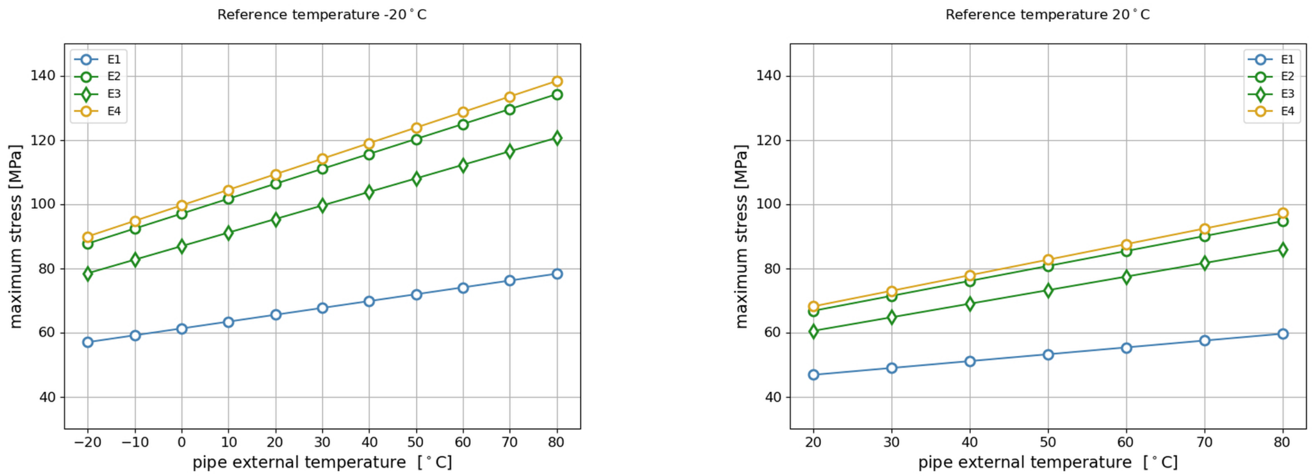

a) for T_{env}=−20°C *b) for* T_{env}=20°C

Fig. 19. Maximal equivalent stress [MPa] in local pipeline route changes, as a function of pipe outer surface temperature for environmental temperature a)−20°C*, b)* 20°C

The value of fatigue strength for a steel of comparable mechanical properties like the one used in the investigated pipeline, according to literature [19], is ca. 170 MPa for the case of bending. This suggests that, under the assumption of lack of stress concentrators within pipes, fatigue damage in pipes should not occur, especially within very low number of cycles.

Locations of observed leakages in the actual pipeline do not overlap with possible locations that can be selected on the basis of the performed structural analysis. In the K1 and K2 compensators, which are the most stressed, no leakage was found. On the contrary, damage was present in the moderately loaded K3-6 compensators. Better agreement can be found in case of E2-4 locations where higher stress levels coincide with the actual leakages. However, the nominal stress levels should not cause any damage. This might suggest that in the investigated case there are other, not revealed yet, factors that lead to a large intensification of fatigue processes and lead finally to pipeline damage despite the lack of alarming nominal stress levels.

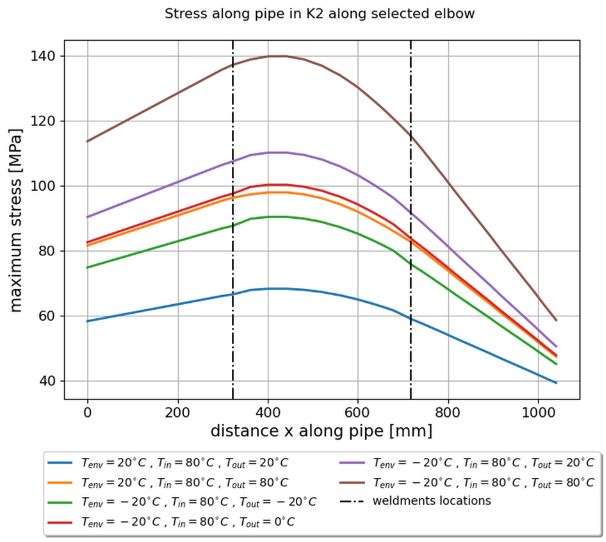

Fig. 20. Maximal stress [MPa] distribution along pipeline in the part depicted in Fig. 17 for selected cases of temperatures. Dash-dotted lines show actual location of welded joints connecting bend with the straight pipes.

6. Reliability aspects of pipeline operation

The analysis of the damage to the pipeline shows that they appeared in characteristic places and independently of each other. In the analysis, the leakage of the pipeline occurring as a result of the propagation of the crack through the whole thickness of the pipe wall was assumed as a failure. All the noted damage was located in the immediate vicinity of the welded joints connecting the bends with straight sections of the pipeline (Fig. 10). Significantly, none of the damage occurred elsewhere in the pipeline. Therefore, it was assumed that in the reliability analysis, the pipeline will be considered as an object consisting of 56 identical elements, operating in the same conditions and which may fail independently of each other. Each pipeline part in the immediate vicinity of the welded joint connecting the bend with the straight section is treated as a single element. The assumed number of elements of the object results from the fact that the entire pipeline has 28 bends, and each of them is connected to straight sections with two welds, each of which constitutes a potential damage area.

With the data on the time of failures occurrence and the time of commencement of operation of the pipeline, the operating times to failure were determined for those of the 56 identified elements that were damaged (Tab. 3). Until the end of the observation, the remaining elements were not damaged and the whole data set was treated as including truncated data.

Table 3. Times till failure of the elements of the pipeline

Element No.	Time till failure [days]
1	945
2	984
3	986
4	1005
5	1014
6	1048
7	1057
8	1064
9	1075
10	1075
11	1075
12-56	>1076 (truncated data)

Based on Tab. 3, the course of the empirical reliability index, which is the failure stream parameter (ω*(Δt)), was determined and presented in Fig. 21.

$$\omega^*(\Delta t) = \frac{n'(\Delta t)}{n_0 \cdot \Delta t} \tag{1}$$

where:

n'(Δt) – number of elements which failed for the first or subsequent time in a given time range Δt,

n_0 – number of elements tested,

Δt – length of the adopted time range.

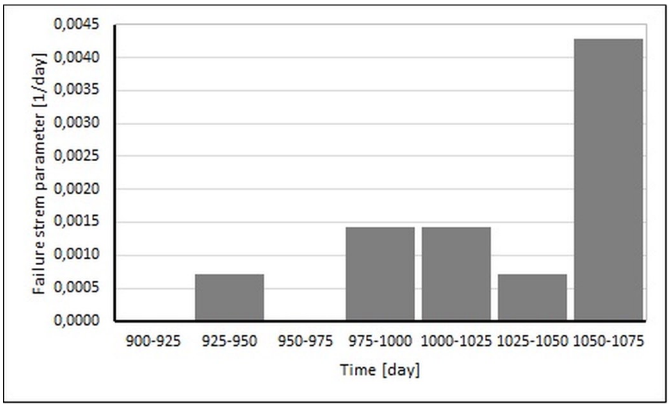

Fig. 21. Failure stream parameter values

The observation of its course shows that after the 925th day of operation, the value of the parameter becomes greater than zero and begins to increase. Generally, such a fact is interpreted as the time the technical object enters the aging period. In this case, the beginning of the increasing course over time can be interpreted as the beginning of the period in which the cracks initiated by corrosion and propagating from the inside of the pipeline, in some elements, already reach a length equal to the wall thickness and cause the failures observed as a pipeline leak. It can be assumed that in the further operation, the number of such failures will increase since the subsequent considered elements will most likely be damaged in the same way, and the observed values of failure stream parameter will continue to increase.

Treating the set of 56 distinguished elements as observed till their first failures, the working times till failure of 11 of them were recorded and the rest were considered as truncated data. On this basis, the Kaplan Meier analysis was performed. The determined graph of the survival function is shown in Fig. 22.

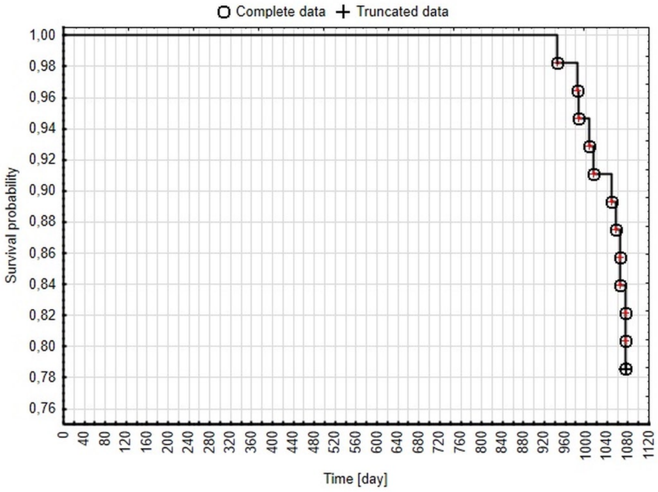

Fig. 22. Survival function for truncated data in the Kaplan-Meier analysis

The graph indicates the probability of surviving without a failure for a certain number of days for each individual element. This value drops very quickly after reaching the operating time of 940 [days]. It can be concluded that each of the remaining available (undamaged) components is less and less likely to survive the next days without a failure. As the probability decreases quickly, it is possible to predict the appearance of many successive failures in the observed set of elements over a short time.

The third stage of the reliability analysis is to determine the probability distribution of operating time till failure for the observed elements. On the basis of the collected data on time till failures and truncated data (Tab. 3), the Weibull distribution was fitted using the Statistica computer program as a mathematical model of the operating time till failure. The parameters determined by the maximum likelihood method are as follows: α = 24.96; β = 1139.6 [days]. The probability density function is presented as [17, 20]:

$$f(t)=\alpha\cdot\left(\frac{1}{\beta}\right)^{\alpha}\cdot t^{\alpha-1}\cdot e^{\left(-\left(\frac{t}{\beta}\right)^{\alpha}\right)} \qquad (2)$$

where:

α – shape parameter,
β – scale parameter.

The initial part of the cumulative distribution function F(t) (for complete data) with the determined 95% confidence interval is presented in Fig. 23.

Next, for the obtained distribution, the course of the forecasted failure probability density function f(t), cumulative distribution function F(t) and failure rate λ(t) were plotted over a period longer than the time adopted for the complete data (Fig. 24, 25).

The graphs show an accumulation of the failure probability density between 1000 and 1200 operation days and a rapid increase in cumulative distribution function values during this time. The determined course of the failure rate shows its characteristic feature which is the intense increase over time. From this fact it can be directly concluded that the probability of failure of each element increases significantly with each subsequent period that it survives without a failure.

The determined changes in the values of the failure stream parameter, the survival function as well as the cumulative distribution function, the failure rate and the expected value of operation time till failure amounting to 1115 [days] allow one to suggest that in order to avoid subsequent failures of the pipeline, appropriate preventive

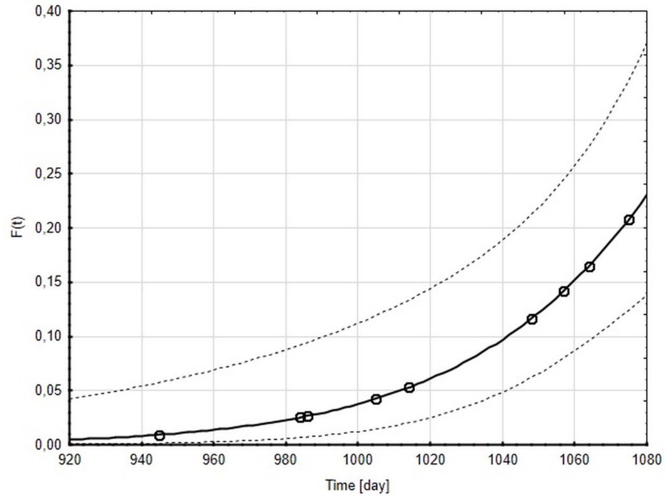

Fig. 23. Cumulative distribution function course for a single pipeline element with 95% confidence interval

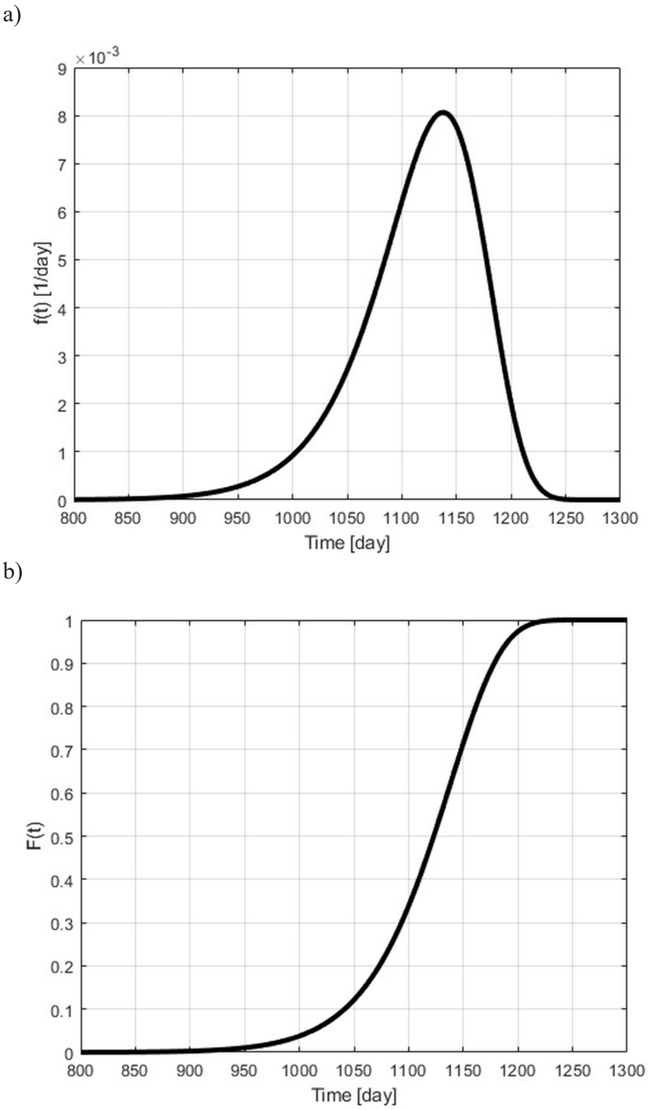

Fig. 24. Failure probability density function a) and cumulative distribution function of the operation time till failure b)

measures should be taken with regard to all available (undamaged) elements, as the probability of failure indicated by the indexes is high and increases rapidly over time. It should be borne in mind that the assumption adopted in the reliability analysis about the crack initiation and propagation in the welded joints areas does not actually have

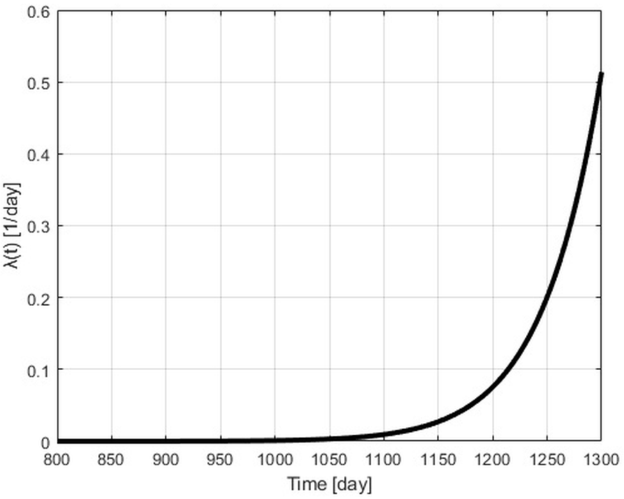

Fig. 25. Failure rate

to take place in each of them. However, due to: the method of making welded joints (without stress relief annealing), aggressive affecting of ammonia water on the pipeline material, high operating temperature and variable stresses, the appearance of a microcrack and its propagation from the inside to the outside of the wall is very likely and confirmed by observations in a number of objects of this type operated in very similar conditions [4, 9]. Hence, the suggested preventive measures in areas where leaks have not yet occurred seem to be the most justified, especially if the costs of carrying them out are lower than the later losses resulting from the failures.

Another possible action is to verify whether a propagating fracture has already appeared in a given area, for which non-destructive ultrasonic testing can be applied. Such tests may be repeated periodically.

7. Conclusions

As a result of the tests of the delivered parts of the high-pressure ammonia water pipeline of the coke oven battery complex, the following conclusions were formulated.

The pipe sections of the tested part of the pipeline were made of low-carbon steel of a chemical composition corresponding to the chemical composition of the steel grade P235GH. The bends in the tested section of the pipeline were manufactured from a material of a different chemical composition than the pipe sections. The B1 bend material has a chemical composition corresponding to the chemical composition of steel grade P245GH. The material of bends A1 and C1 has a chemical composition corresponding to the chemical composition of steel grade P250GH.

The circumferential welded joints were made by arc welding. The external appearance of the welds raises the following reservations: variations in the shape of the weld face are observed, the occurrence of asymmetry of the joint was found (it is bound with unequal folding of the sections of the pipeline welded together), metal spattering appears on the outer surface of the pipes welded, and unevenness of the weld root was found.

Transverse cracks (in relation to the pipeline axis) appear in the area of the welded joints. They are located in the material of the bends outside the heat-affected zone. Cracks propagated from the inside of the bends, and some of them covered the entire thickness of the pipeline wall. As a result, leaks appeared in these places and the necessity to put on sealing bands.

It may be assumed that it was the incorrectly made welded joints that caused excessive tensile stresses in the surrounding material. These stresses present in the object operating in the corrosive environment, which is the medium flowing through the pipeline, led to the formation of damage and leakage of the pipeline. On the basis of the conducted tests and the obtained results, it is difficult to unequivocally state what was the cause and whether there was only one cause of the failures. The structural analysis of pipeline compensators led to similar conclusions.

The statistical and reliability analyses of the failures occurrence suggest that in the considered case certain preventive actions should be performed to avoid the subsequent failures of the pipeline.

A recommendation affecting the safe operation of ammonia water pipelines is monitoring the tightness of compensators after 1000 days of operation.

Another recommendation, developed on the basis of the reliability characteristics of the tested pipeline structure, is the necessity to quickly repair all endangered parts of the structure after detecting the first damage to the pipeline.

References

1. Abedi S. Sh., Abdolmaleki A., Adibi N. Failure analysis of SCC and SRB induced cracking of a transmission oil products pipeline. Engineering Failure Analysis, 2007; 14 (1): 250–261, https://doi.org/10.1016/j.engfailanal.2005.07.024.
2. Aljoboury A., Mourad A., Alawar A., Abou Zour M., Abuzeid O. Stress corrosion cracking of stainless steels recommended for building brine recirculation pumps. Engineering Failure Analysis, 2010; 17 (6): 1337–1344, https://doi.org/10.1016/j.engfailanal.2010.03.008.
3. ASM Handbook. Volume 13C, Corrosion: Environments and Industries. ASM INTERNATIONAL, 2006, doi: 10.31399/asm.hb.v13c.9781627081849.
4. Banaszek A., Łosiewicz Z., Jurczak W. Corrosion Influence on Safety of Hydraulic Pipelines Installed on Decks of Contemporary Product and Chemical Tankers. Polish Maritime Research, 2018; 25 (2): 71–77, https://doi.org/10.2478/pomr-2018-0056.
5. Borucka A. Method of testing the readiness of means of transport with the use of semi-Markov processes, Transport 2021; 36 (1), https://doi.org/10.3846/transport.2021.14370
6. Borucka, A. Three-state Markov model of using transport means. Business Logistics In Modern Management, 2018; 3-19.
7. Campione G., Giambanco G. Influence of design mistakes and material degradation on the collapse of a long-span RC roof in South Italy. Engineering Failure Analysis, 2020; 111, https://doi.org/10.1016/j.engfailanal.2019.104257.
8. Cao Y., Chang Q., Zhen Y. Numerical simulation of fracture behavior for the pipeline with girth weld under axial load. Engineering Failure Analysis, 2022; 136, https://doi.org/10.1016/j.engfailanal.2022.106221.
9. Dobosiewicz J., Brunné W. Przyczyny nieszczelności rurociągu wody amoniakalnej w obszarze połączeń spawanych. Causes of pipeline leakage ammonia water near to welded joints. Przegląd Spawalnictwa, 2011; 83 (7): 14–16, https://doi.org/10.26628/ps.v83i7.530
10. Documentation of the project U-28062. Object 251 Inter-raw gas network. High ammonia-water piping.
11. Hafez K. M. The role of a plain dent on the failure mode of a crude oil pipeline. Engineering Failure Analysis, 2021; 122, https://doi.org/10.1016/j.engfailanal.2021.105291.
12. Khosravani M., Božić Ž., Zolfagharian A., Reinicke T. Failure analysis of 3D-printed PLA components: Impact of manufacturing defects and thermal ageing. Engineering Failure Analysis, 2022; 136, https://doi.org/10.1016/j.engfailanal.2022.106214.
13. Kozłowski E., Borucka A., Swiderski A., Gil, L. Predicting the Fatigue Life of a Ball Joint. Transport and Telecommunication, 2021; 22(4): 453-460, doi:10.2478/ttj-2021-0035

14. Mistur L. Spawanie i napawanie w naprawach części maszyn i konstrukcji metalowych. Wydaw. i Handel Książkami “KaBe”, Krosno 2003.
15. Movafeghi A., Mohammadzadeh N., Yahaghi E. et al. Defect Detection of Industrial Radiography Images of Ammonia Pipes by a Sparse Coding Model. Journal of Nondestructive Evaluation, 2018; 37(3), https://doi.org/10.1007/s10921-017-0458-9.
16. Nyborg R., Lunde, L. Measures for reducing SCC in anhydrous ammonia storage tanks. Process Safety Progress, 1996; 15 (1): 32–41, doi: 10.1002/prs.680150110.
17. Pham H. (ed.). Handbook of Reliability Engineering. Springer-Verlag, London, 2003. https://doi.org/10.1007/b97414
18. Schweitzer P. (ed.). Carbon steel and low alloy steel in corrosion and corrosion protection handbook. Marcel Dekker, New York 1983.
19. Skoć A., Spałek J. Podstawy Konstrukcji Maszyn, Vol. 1, WNT, Warszawa 2006.
20. Tobias P. A., Trindade D. C. Applied Reliability. Third Edition. CRC Press Taylor & Francis Group, Boca Raton, 2012.
21. Wang W., Zhang Y., Li Y., Hu Q., Liu C., Liu C. Vulnerability analysis method based on risk assessment for gas transmission capabilities of natural gas pipeline networks. Reliability Engineering & System Safety, 2022; 218 (B), https://doi.org/10.1016/j.ress.2021.108150.
22. Zhu L., Luo J., Wu G., Han J., Chen Y., Song C. Study on strain response of X80 pipeline steel during weld dent deformation. Engineering Failure Analysis, 2021; 123, https://doi.org/10.1016/j.engfailanal.2021.105303.